

# Electron-Ion Collider impact study on the tensor charge of the nucleon

Leonard Gamberg<sup>a</sup>, Zhong-Bo Kang<sup>b,c,d</sup>, Daniel Pitonyak<sup>e</sup>, Alexei Prokudin<sup>a,f</sup>, Nobuo Sato<sup>f</sup>, Ralf Seidl<sup>g</sup>

<sup>a</sup>Division of Science, Penn State University Berks, Reading, Pennsylvania 19610, USA

<sup>b</sup>Department of Physics and Astronomy, University of California, Los Angeles, California 90095, USA

<sup>c</sup>Mani L. Bhaumik Institute for Theoretical Physics, University of California, Los Angeles, California 90095, USA

<sup>d</sup>Center for Frontiers in Nuclear Science, Stony Brook University, Stony Brook, New York 11794, USA

<sup>e</sup>Department of Physics, Lebanon Valley College, Annville, PA 17003, USA

<sup>f</sup>Theory Center, Jefferson Lab, 12000 Jefferson Avenue, Newport News, Virginia 23606, USA

<sup>g</sup>RIKEN BNL Research Center, Upton, New York 11973, USA

---

## Abstract

In this letter we study the impact of the Electron-Ion Collider (EIC) on the phenomenological extraction of the tensor charge from a QCD global analysis of single transverse-spin asymmetries (SSAs). We generate EIC pseudo-data for the Collins effect in semi-inclusive deep-inelastic scattering for proton and  $^3\text{He}$  beams across multiple center-of-mass energies. We find a significant reduction in the uncertainties for the up, down, and isovector tensor charges that will make their extraction from EIC data on SSAs as or more precise than current lattice QCD calculations. We also analyze the constraints placed by future data from the proposed SoLID experiment at Jefferson Lab.

---

## 1. Introduction

The tensor charge  $g_T$  is one of the fundamental charges of the nucleon [1–5] and, arguably, the least known. The uniqueness of  $g_T$  is also that it sits at the intersection of three key areas of nuclear physics: 3-dimensional tomography of the nucleon (see, e.g., [6–13]), searches for beyond the Standard Model (BSM) physics (see, e.g., [14–16]), and *ab initio* approaches like lattice QCD or Dyson-Schwinger Equations (see, e.g., [17–20]). The focus of this letter will be on accessing the tensor charge through the first avenue, namely, an analysis of single transverse-spin asymmetries (SSAs) that are sensitive to the 3-dimensional structure of the nucleon. In particular, one can compute  $g_T$  from an integral of the transversity parton distribution function (PDF)  $h_1(x)$  [1–5] over the parton momentum fraction  $x$ :

$$g_T = \delta u - \delta d \quad \text{where} \quad \delta u = \int_0^1 dx (h_1^u(x) - h_1^{\bar{u}}(x)), \quad \delta d = \int_0^1 dx (h_1^d(x) - h_1^{\bar{d}}(x)), \quad (1)$$

while  $u$  and  $d$  represent up and down quarks, respectively.

Phenomenological extractions of the tensor charge have typically fallen into two main categories. The first are those studies that use transverse momentum dependent (TMD) observables like the Collins effect in semi-inclusive deep-inelastic scattering (SIDIS) [21–27] and semi-inclusive electron-positron annihilation to almost back-to-back hadrons (SIA) [28–32], which allow for the transversity TMD PDF  $h_1(x, k_T^2)$  and Collins TMD fragmentation function (FF)  $H_1^+(z, p_T^2)$  (defined below) to be fit simultaneously [6, 9, 12, 13]. We note that the Collins effect for hadron-in-jet measurements from proton-proton collisions is also sensitive to the coupling of  $h_1(x, k_T^2)$  and  $H_1^+(z, p_T^2)$  [33–36]. In addition, one can use Generalized Parton Distributions (GPDs) to extract the tensor charge [7]. The second category is those analyses that use dihadron observables in SIDIS [37–40], SIA [41], and proton-proton collisions [42, 43],

---

*Email addresses:* lpg10@psu.edu (Leonard Gamberg), zkang@g.ucla.edu (Zhong-Bo Kang), pitonyak@lvc.edu (Daniel Pitonyak), prokudin@jlab.org (Alexei Prokudin), nsato@jlab.org (Nobuo Sato), rseidl@ribf.riken.jp (Ralf Seidl)

where the collinear transversity PDF  $h_1(x)$  and dihadron FF  $H_1^\zeta(z, M_h)$  can be fit simultaneously [8, 10, 11]. Generally the extraction of the tensor charge from both the TMD (SIDIS+SIA) and dihadron approaches [6, 8–12] have shown tension with lattice QCD calculations at the physical point [17, 18, 20]. However, we note the study in Ref. [44] found that there do exist solutions for  $h_1(x, k_T^2)$  and  $H_1^\perp(z, p_T^2)$  that can successfully describe both Collins effect SIDIS measurements and lattice data.

Moreover, there was a recent global analysis of SSAs performed in Ref. [13] (JAM20), which included not only Collins effect SIDIS and SIA data but also Sivers effect SIDIS and Drell-Yan measurements [22, 24–27, 45–48] as well as proton-proton  $A_N$  data [49–52]. The JAM20 results found for the first time an agreement between experimental data and lattice QCD (without including lattice data in the fit) for  $\delta u$ ,  $\delta d$ , and  $g_T$ , as calculated in Eq. (1). The crucial aspect that allowed for such an agreement was the inclusion of  $A_N$  data. This observable is *collinear* twist-3 [53–58] and dominated by a term that couples  $h_1(x)$  to the quark-gluon-quark FFs  $H_1^{\perp(1)}(z)$  and  $\tilde{H}(z)$  [13, 59, 60]. The function  $H_1^{\perp(1)}(z)$  is the first moment of the Collins TMD FF, and  $\tilde{H}(z)$  generates the  $P_{hT}$ -integrated SIDIS  $A_{UT}^{\sin\phi_S}$  asymmetry, where  $P_{hT}$  is the transverse momentum of the hadron w.r.t. the momentum of the virtual photon, by again coupling with  $h_1(x)$  [61].

Furthermore, the JAM20 results, due to the inclusion of  $A_N$  data, also give the most precise phenomenological extraction of  $g_T$  to date:  $g_T = 0.87(11)$ . Nevertheless, the error in  $g_T$ , along with those for  $\delta u, \delta d$  (JAM20 values are  $\delta u = 0.72(19), \delta d = -0.15(16)$ ) are still much larger ( $\sim 12\%$  for  $g_T$ ,  $\sim 25\%$  for  $\delta u$ , and  $\sim 100\%$  for  $\delta d$ ) than the uncertainties from lattice QCD calculations ( $\lesssim 5\%$  for all of  $\delta u, \delta d$ , and  $g_T$ ) [17, 18, 20]. The main cause of the uncertainty for phenomenological computations is that they rely on integrals of  $h_1(x)$  over the entire  $x$  region from 0 to 1 (see Eq. (1)). However, current SIDIS measurements only cover a region  $0.02 \lesssim x \lesssim 0.3$ . This leaves the transversity PDF basically unconstrained in the small- $x$  and large- $x$  regimes. The inclusion of  $A_N$  data does give some further constraints in the larger- $x$  region since in that observable one integrates from  $x_{min}$  to 1, where  $0.2 \lesssim x_{min} \lesssim 0.7$ . We also mention that a first principles calculation of the small- $x$  asymptotics of the valence transversity TMD PDF has been performed in Ref. [62]. Nevertheless, one clearly needs very precise data at both  $x \lesssim 0.02$  and  $x \gtrsim 0.3$  in order to significantly reduce the uncertainties in phenomenological extractions of the tensor charge.

The future Electron-Ion Collider (EIC) [63, 64] at Brookhaven National Laboratory will make the most precise SIDIS measurements at small  $x$  (down to  $x \sim 10^{-4}$ ) while also increasing the precision of the data in the region up to  $x \sim 0.3$ . The 12 GeV program currently underway at Jefferson Lab (JLab) [65] will make precision measurements up to  $x \sim 0.6$ . In terms of the tensor charge, future data from the proposed SoLID experiment [66] will offer the tightest constraints in this large- $x$  region. The goal of this letter is to perform an impact study of future EIC data on the tensor charge of the nucleon using the JAM20 results as a baseline. In Sec. 2 we discuss the EIC pseudo-data used in the analysis. This includes both proton and  $^3\text{He}$  beams across multiple center-of-mass (CM) energies. In Sec. 3 we include these pseudo-data in the global analysis of Ref. [13] and, from the newly extracted transversity PDF, compute the tensor charges  $\delta u, \delta d$ , and  $g_T$  and compare them to those of recent lattice QCD calculations. In addition, since the proposed SoLID experiment itself would give significant impact on the tensor charge at large  $x$ , we perform a similar analysis on its pseudo-data [67]. Finally, we summarize our results and discuss the future outlook in Sec. 4.

## 2. Generating EIC Pseudo-Data

The EIC will provide data sensitive to the transversity PDF through SSAs in single-hadron and dihadron reactions. For the former, measurements will be made of the Collins effect  $A_{UT}^{\sin(\phi_h+\phi_S)}$  in  $e + N^\uparrow \rightarrow e + h + X$ , where  $\phi_h$  ( $\phi_S$ ) is the azimuthal angle of the outgoing hadron momentum (nucleon transverse spin) vector w.r.t. the lepton scattering plane. We generated EIC pseudo-data for both transversely polarized proton and  $^3\text{He}$  beams with charged pions detected in the final state and applied the JAM20 cuts of  $0.2 < z < 0.6$ ,  $Q^2 > 1.63 \text{ GeV}^2$ , and  $0.2 < P_{hT} < 0.9 \text{ GeV}$ . Table 1 summarizes the data used in our fit, which includes a total of 8223 EIC pseudo-data points on the Collins effect in SIDIS plus the 517 SSA data points in the original JAM20 global analysis. The EIC pseudo-data covers multiple CM energies  $\sqrt{S}$  based on the energy of the electron beam  $E_e$  and nucleon beam  $E_N$ :  $\sqrt{S} \approx 2\sqrt{E_e E_N}$ . The pseudo-data was generated with pythiaRHIC [68] that uses PYTHIA 6.4 [69] as an event generator. Realistic EIC detector acceptances and momentum smearing were implemented via the eic-smear package [70] and is predominantly based on the expected resolutions that are discussed in the EIC handbook [71]. For pion identification, the momentum and rapidity ranges that evolved from the EIC user group Yellow Report effort were used. The proton and  $^3\text{He}$  polarizations

EIC Pseudo-data			
Observable	Reactions	CM Energy ( $\sqrt{S}$ )	$N_{\text{pts.}}$
Collins (SIDIS)	$e + p^\uparrow \rightarrow e + \pi^\pm + X$	141 GeV	756 ( $\pi^+$ ) 744 ( $\pi^-$ )
		63 GeV	634 ( $\pi^+$ ) 619 ( $\pi^-$ )
		45 GeV	537 ( $\pi^+$ ) 556 ( $\pi^-$ )
		29 GeV	464 ( $\pi^+$ ) 453 ( $\pi^-$ )
	$e + {}^3\text{He}^\uparrow \rightarrow e + \pi^\pm + X$	85 GeV	647 ( $\pi^+$ ) 650 ( $\pi^-$ )
		63 GeV	622 ( $\pi^+$ ) 621 ( $\pi^-$ )
		29 GeV	461 ( $\pi^+$ ) 459 ( $\pi^-$ )
		<b>Total EIC <math>N_{\text{pts.}}</math></b>	<b>8223</b>

JAM20 [13]			
Observable	Reactions	Experimental Refs.	$N_{\text{pts.}}$
Sivers (SIDIS)	$e + (p, d)^\uparrow \rightarrow e + \pi^\pm/\pi^0 + X$	[22, 25, 45]	126
Sivers (DY)	$\pi^- + p^\uparrow \rightarrow \mu^+ + \mu^- + X$	[48]	12
Sivers (DY)	$p^\uparrow + p \rightarrow W^\pm/Z + X$	[46]	17
Collins (SIDIS)	$e + (p, d)^\uparrow \rightarrow e + \pi^\pm/\pi^0 + X$	[22, 23, 25]	126
Collins (SIA)	$e^+ + e^- \rightarrow \pi^+ + \pi^- + X$	[28–31]	176
$A_N$	$p^\uparrow + p \rightarrow \pi^\pm/\pi^0 + X$	[49–52]	60
<b>Total JAM20 <math>N_{\text{pts.}}</math></b>			<b>517</b>

Table 1: Summary of the data used in our analysis, including the number of points ( $N_{\text{pts.}}$ ) in each reaction. (Top) EIC pseudo-data for the Collins effect in SIDIS for different polarized beam types, CM energies, and final states. (Bottom) Data used in the original JAM20 global analysis of SSAs.

were assumed to be 70%, and the uncertainties were scaled to accumulated luminosities of  $10 \text{ fb}^{-1}$ . In the case of  ${}^3\text{He}$ , it was assumed that the two protons can be tagged in the very forward instrumentation, and was thus simulated by generating  $e + n^\uparrow$  data after taking into account the neutron polarization in  ${}^3\text{He}$ . The uncertainties on the expected SSAs were evaluated by re-weighting the unpolarized simulations based on the phenomenological results of Ref. [72] and extracting the reconstructed asymmetries. As a crude measure of detector smearing and acceptance effects in a real detector, the differences between extracted asymmetries using perfectly tracked and smeared values were assigned as systematic uncertainties. This tries to conservatively mimic the uncertainties that may be related to the unfolding of smearing and particle mis-identification in an actual detector. In addition, we separately assess the impact from Collins effect SIDIS pseudo-data from SoLID (for the “enhanced” scenario) [67]. We note that precision measurements from Belle II on the Collins effect in SIA will have impact on the tensor charge due to reducing the uncertainties in the Collins TMD FF [73]. However, we do not consider this in our study, as current data already constrain the Collins function rather well [28–31].

### 3. Phenomenological Results

We begin by briefly discussing the methodology of the JAM20 global analysis, which serves as the baseline for our impact study, and refer the reader to Ref. [13] for more details. We employ a Gaussian parametrization for the

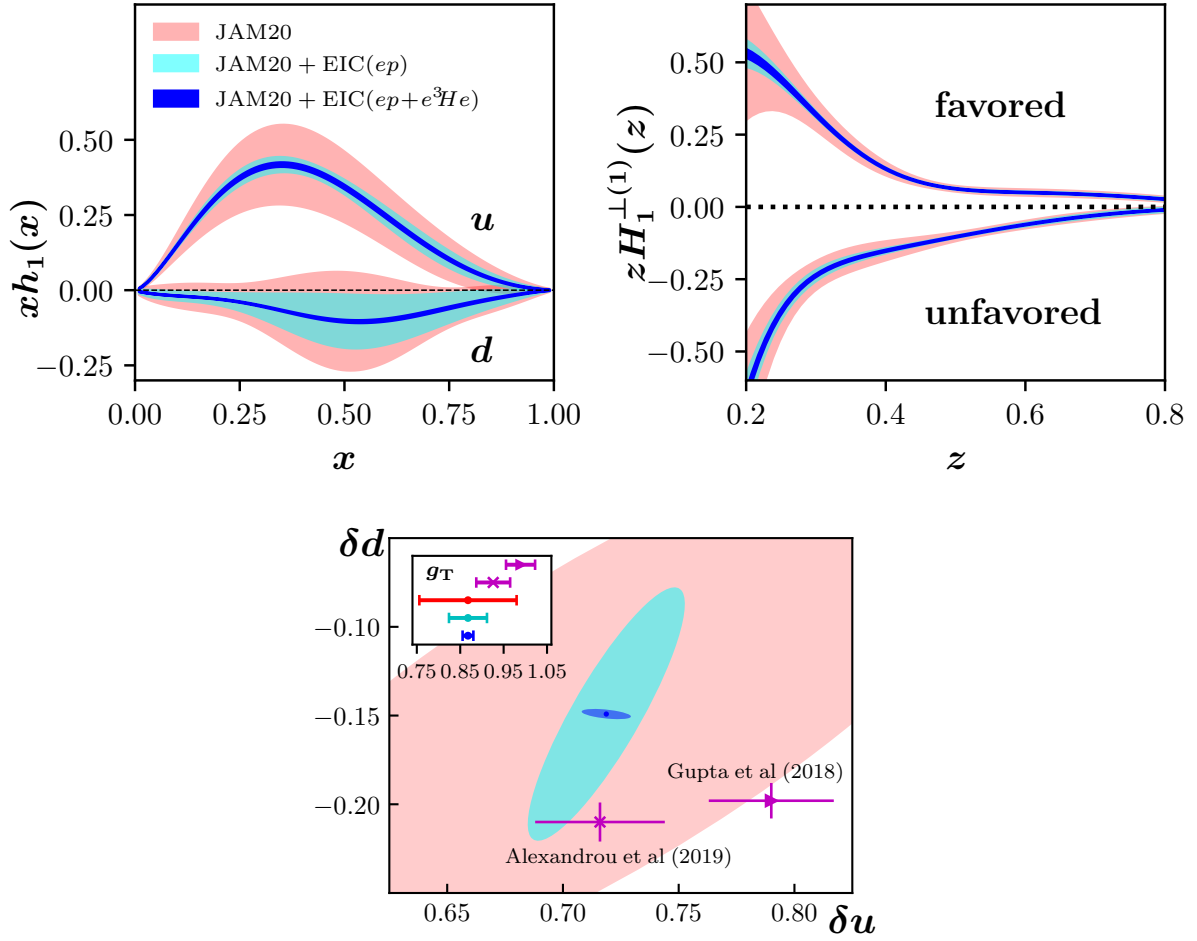


Figure 1: (Top) Plot of the transversity function for up and down quarks as well as the favored and unfavored Collins function first moment from the JAM20 global analysis [13] (light red band) as well as a re-fit that includes EIC Collins effect pion production pseudo-data for a proton beam only (cyan band) and for both proton and  $^3He$  beams together (blue band). (Bottom) Individual flavor tensor charges  $\delta u$ ,  $\delta d$  as well as the isovector charge  $g_T$  for the same scenarios. Also shown are the results from two recent lattice QCD calculations [18, 20] (purple). All results are at  $Q^2 = 4 \text{ GeV}^2$  with error bands at 1- $\sigma$  CL.

transverse momentum dependence of the TMD PDFs and FFs. In particular, for the transversity TMD PDF we have

$$h_1^q(x, k_T^2) = h_1^q(x) \frac{1}{\pi \langle k_T^2 \rangle_{h_1}^q} \exp\left[-\frac{k_T^2}{\langle k_T^2 \rangle_{h_1}^q}\right], \quad (2)$$

with  $q$  being a quark flavor, and  $\langle k_T^2 \rangle_{h_1}^q$  the transverse momentum width. Note that  $\vec{k}_T$  is the transverse momentum of the struck quark. For  $h_1^q(x)$  we only allow  $q = u, d$  and explicitly set antiquark functions to zero. Even though an important goal of the EIC will be to constrain the sea quark transversity PDFs, for the tensor charge their inclusion is expected to have a small effect. Lattice QCD finds that contributions from disconnected diagrams to the tensor charge are about two orders of magnitude smaller than connected diagrams [18, 20]. In addition, if one assumes a symmetric sea, then antiquark contributions cancel when calculating  $g_T$ , as one can see from Eq. (1). The Collins TMD FF is

parametrized as

$$H_1^{\perp h/q}(z, p_T^2) = \frac{2z^2 M_h^2}{\pi \langle p_T^2 \rangle_{H_1^{\perp}}^{h/q}} H_1^{\perp(1)}(z) \exp\left[-\frac{p_T^2}{\langle p_T^2 \rangle_{H_1^{\perp}}^{h/q}}\right], \quad (3)$$

where  $z$  is the hadron momentum fraction,  $\langle p_T^2 \rangle_{H_1^{\perp}}^{h/q}$  is the transverse momentum width, and  $M_h$  is the produced hadron mass. Note that  $\vec{p}_T$  is the transverse momentum of the produced hadron with respect to the fragmenting parton. We allow for favored and unfavored Collins functions.

Our study was conducted using roughly 200 replicas from the JAM20 analysis as priors in a fit of all the data in Table 1 (8740 total points). The results for the impact on the up and down transversity PDF  $h_1(x)$  as well as the Collins function first moment  $H_1^{\perp(1)}(z)$  are shown in the top panel of Fig. 1. One clearly sees a drastic reduction in the transversity uncertainty band once EIC data is included compared to the original JAM20 results. Even the uncertainties for the Collins function decrease noticeably in the smaller- $z$  region. This will allow for a more stringent test of the universality of the Collins function between SIDIS, electron-positron annihilation, and proton-proton collisions [74–80]. We emphasize that the  ${}^3\text{He}$  data is crucial for a precise determination of the down quark transversity PDF and for up and down flavor separation, enabling a higher decorrelation between  $\delta u$  and  $\delta d$ . Specifically, the Pearson correlation coefficients were found to be

$$\rho[\delta u, \delta d] \equiv \frac{\langle \delta u \cdot \delta d \rangle - \langle \delta u \rangle \langle \delta d \rangle}{\Delta(\delta u) \Delta(\delta d)} = \begin{cases} 0.80 & \text{for JAM20,} \\ 0.87 & \text{for JAM20 + EIC}(ep), \\ -0.48 & \text{for JAM20 + EIC}(ep+e^3\text{He}), \end{cases}$$

where  $\langle \dots \rangle$  is the average value over all replicas, and  $\Delta(\dots)$  is the uncertainty (standard deviation) of the calculated tensor charge. (The correlation coefficient  $\rho$  can be in the range  $[-1, 1]$ , where  $\rho = \pm 1$  indicates 100% correlation (anti-correlation) and  $\rho = 0$  indicates zero correlation.) Moreover, the well-constrained up and down  $h_1(x)$  translate into very precise calculations of  $\delta u$ ,  $\delta d$ , and  $g_T$ , as shown in the bottom panel of Fig. 1. We find all relative errors are now  $\lesssim 2\%$ :  $\delta u = 0.719(11)$ ,  $\delta d = -0.149(3)$ ,  $g_T = 0.868(12)$ . From the two lattice QCD calculations at the physical point [18, 20] that are also included in that plot, we can conclude that EIC data will allow for phenomenological extractions of the tensor charges to be as, or more precise than current lattice results. Thus, the EIC will provide a unique opportunity to explore the possible tension between these two approaches discussed in Ref. [10].

In order to better understand which kinematic regions are most important for a precise extraction of the tensor charge  $g_T$  to be possible (like we find in the bottom panel of Fig. 1), we calculate the sensitivity coefficients [81, 82]  $S[A_{UT}^{\sin(\phi_h+\phi_s)}, h_1^{u-d}]$  for the transversity isovector combination  $h_1^{u-d} \equiv (h_1^u - h_1^d)$ , generically defined as

$$S[O, f] \equiv \frac{\langle O \cdot f \rangle - \langle O \rangle \langle f \rangle}{(\Delta O)_{\text{EIC}} (\Delta f)_{\text{JAM20}}}, \quad (4)$$

where  $(\Delta O)_{\text{EIC}}$  is the EIC uncertainty for the observable  $O$ , and  $(\Delta f)_{\text{JAM20}}$  is the JAM20 theoretical uncertainty for the function  $f$ . The larger the sensitivity coefficient  $S$ , the larger the impact of the new data set on the observable. We note that  $A_{UT}^{\sin(\phi_h+\phi_s)}$  is a function of  $(x, Q^2, z, P_{hT})$  while  $h_1^{u-d}$  is only a function of  $(x, Q^2)$ . Therefore, we define the following average sensitivity coefficient for each  $(x, Q^2)$  bin:

$${}^D S[A_{UT}^{\sin(\phi_h+\phi_s)}, h_1^{u-d}] \equiv \frac{1}{N_{\text{bin}}} \sum_i S_i[A_{UT}^{\sin(\phi_h+\phi_s)}, h_1^{u-d}], \quad (5)$$

where the sum runs over all points  $N_{\text{bin}}$  in a given  $(x, Q^2)$  bin, including all  $(z, P_{hT})$  points in that bin for both  $\pi^+$  and  $\pi^-$  final states. The results for  ${}^D S[A_{UT}^{\sin(\phi_h+\phi_s)}, h_1^{u-d}]$  are shown in Fig. 2 for various CM energies for both proton and  ${}^3\text{He}$  beams. We find that the small- $x$ , small- $Q^2$  region has the most impact on  $h_1^{u-d}$  and, consequently,  $g_T$ . This is reasonable given that current SIDIS data sits at  $x \gtrsim 0.02$  and lower- $Q^2$  data better constrain the non-perturbative features of TMDs. For the proton beam in the left panel of Fig. 2, the highest CM energy ( $\sqrt{S} = 141$  GeV) is the most important in this respect, although the lower CM energies still offer important coverage in this region with some

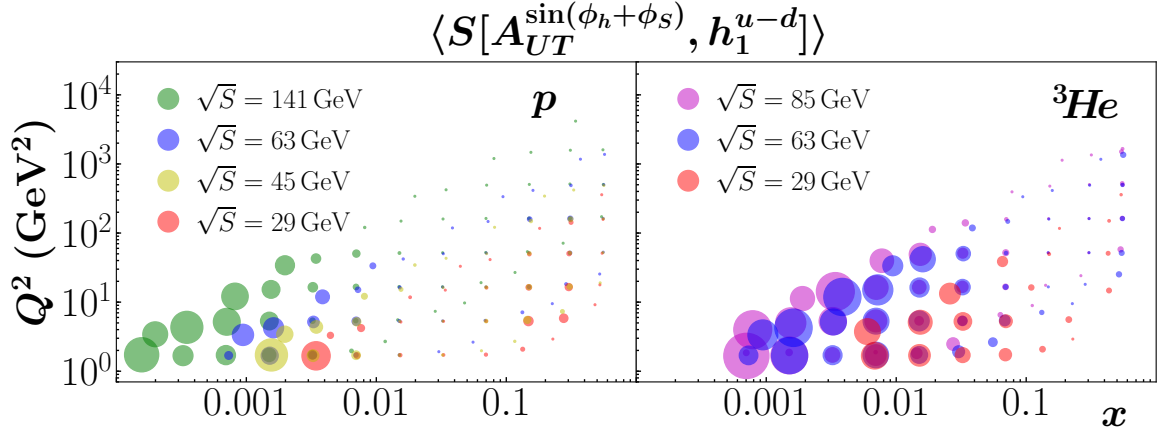


Figure 2: The average sensitivity coefficients  $\langle S[A_{UT}^{\sin(\phi_h+\phi_S)}, h_1^{u-d}] \rangle$  as defined in Eq. (5) for both proton (left) and  ${}^3\text{He}$  (right) beams for various CM energies. The size of the symbols is proportional to the value of sensitivity coefficient.

sizable sensitivity coefficients. We clearly see again in the right panel of Fig. 2 the importance of the  ${}^3\text{He}$  program at the EIC for the extraction of the tensor charge. All CM energies in that case give sizable sensitivity coefficients up to  $x \lesssim 0.02$ . Even though the large- $x$ , large- $Q^2$  region in Fig. 2 shows small sensitivity coefficients, we emphasize the importance of the tremendous  $Q^2$  lever arm of the EIC to help constrain TMD evolution and study the interplay between TMD and collinear approaches.

In addition, we analyze the impact of pseudo-data from the proposed SoLID experiment at JLab [67], since it will potentially offer the tightest constraints in the large- $x$  region [66], and compare the results to the EIC case. SoLID will cover a region of  $0.05 \lesssim x \lesssim 0.65$  and  $1 \lesssim Q^2 \lesssim 8 \text{ GeV}^2$ . After the JAM20 data cuts, our study included 526 points for  $e + p^\uparrow \rightarrow e + \pi^\pm + X$  (311 for  $\pi^+$  and 215 for  $\pi^-$ ) and 696 points for  $e + {}^3\text{He}^\uparrow \rightarrow e + \pi^\pm + X$  (412 for  $\pi^+$  and 284 for  $\pi^-$ ). The SoLID experiment will use both 8.8 GeV and 11 GeV electron beams (CM energy of  $\sqrt{S} = 4.17 \text{ GeV}$  and  $\sqrt{S} = 4.64 \text{ GeV}$ , respectively) for both proton ( $\text{NH}_3$ ) and  ${}^3\text{He}$  targets. Using the tentatively approved running times for both energies and targets, the accumulated luminosities will far exceed the EIC luminosities [67]. Both EIC and SoLID will be systematics limited in most of their covered kinematic ranges.

In the left panel of Fig. 3, we present  $g_T^{[x_{min}]}$  vs.  $x_{min}$ , where  $g_T^{[x_{min}]}$  is the following truncated integral:

$$g_T^{[x_{min}]} \equiv \int_{x_{min}}^1 dx (h_1^u(x) - h_1^d(x)) - (h_1^d(x) - h_1^u(x)) \Big|_{x_{min}}^1. \quad (6)$$

From this quantity, we see that the current JAM20 result only constrains the tensor charge down to  $x \sim 0.1$ , which accounts for about 75% of the total  $g_T$ . Thus, one clearly needs the small- $x$  data at the EIC to fully and precisely determine  $g_T$ , as Fig. 3 highlights. Also shown is the reduction in the error of this quantity from the baseline fit of JAM20. The SoLID experiment does give a significant decrease in the error band as well. With SoLID, one can expect the uncertainty to reduce to 30% of the current JAM20 uncertainty whereas with the EIC the uncertainty will go down to 10% of JAM20. One also notices that  $g_T^{[x_{min}]}$  begins to saturate around  $x \sim 0.01$ , suggesting that very little tensor charge exists at small  $x$ . This observation is consistent with the calculation in Ref. [62] of the small- $x$  asymptotic behavior of the valence transversity TMD PDF. In the right panel of Fig. 3, we see a comparison between SoLID and the EIC for  $\delta u$ ,  $\delta d$ , and the full  $g_T$ . From this plot, we can conclude that SoLID data will also allow for phenomenological extractions of the tensor charges to have similar precision as current lattice results, with relative errors of  $\lesssim 7\%$ :  $\delta u = 0.72(3)$ ,  $\delta d = -0.150(10)$ ,  $g_T = 0.87(4)$ . In addition, SoLID will offer needed complementary measurements to the EIC in order to test that a consistent picture emerges across multiple experiments on the extracted value of the tensor charge. Only when a bulk of experiments give consistent central values for quantities of interest, like the tensor charge, can one claim to have accurate results.

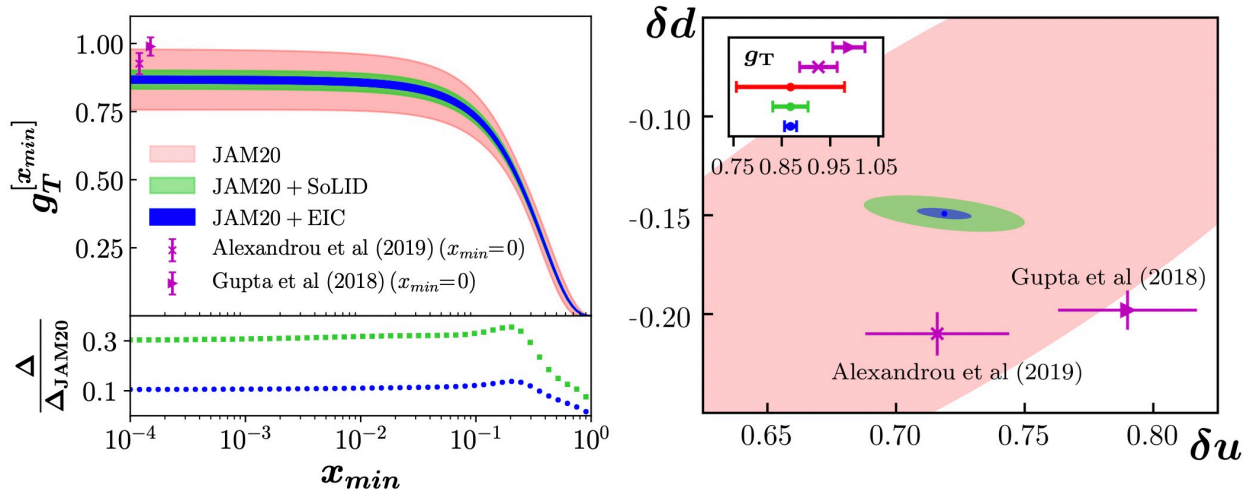


Figure 3: (Left) Plot of the truncated integral (as defined in Eq. (6))  $g_T^{[x_{min}]}$  vs.  $x_{min}$  for the JAM20 global analysis [13] (light red band) as well as a re-fit that includes Collins effect pion production pseudo-data (proton and  ${}^3\text{He}$  together) from SoLID (green band) and for the EIC (blue band). The plot also contains two recent lattice QCD calculations [18, 20]. Note that these lattice data points are for the full  $g_T$  integral (i.e.,  $x_{min} = 0$ ) and have been offset for clarity. Also shown is the ratio  $\Delta/\Delta_{\text{JAM20}}$  of the uncertainty in  $g_T^{[x_{min}]}$  for the re-fit that includes pseudo-data from SoLID (green squares) and for the one that includes pseudo-data from the EIC (blue circles) to that of the original JAM20 fit [13]. That is,  $\Delta$  in the numerator is either  $\Delta_{\text{JAM20+SoLID}}$  (for the case of the green squares) or  $\Delta_{\text{JAM20+EIC}}$  (for the case of the blue circles). (Right) Individual flavor tensor charges  $\delta u, \delta d$  as well as the isovector charge  $g_T$  for the same scenarios. All results are at  $Q^2 = 4 \text{ GeV}^2$  with error bands at  $1\text{-}\sigma$  CL.

#### 4. Conclusion

In this letter, we have studied the impact on the tensor charge from EIC pseudo-data of the SIDIS Collins effect using the results of the JAM20 global analysis of SSAs [13]. Both transversely polarized proton and  ${}^3\text{He}$  beams are considered across multiple CM energies for charged pions in the final state. We find that the EIC will drastically reduce the uncertainty in both the individual flavor tensor charges  $\delta u, \delta d$  as well as their isovector combination  $g_T$ . The  ${}^3\text{He}$  data is especially crucial for a precise determination of the down quark transversity TMD PDF and for up and down flavor separation. Consequently, the EIC will allow for phenomenological extractions of the tensor charges to be as, or more precise than current lattice QCD calculations. This will ultimately show whether a tension exists between experimental and lattice data. In addition, we performed a similar study on SoLID pseudo-data of the SIDIS Collins effect and found that the proposed experiment at Jefferson Lab will also significantly decrease the uncertainty in the tensor charge. Given that the tensor charge is a fundamental charge of the nucleon and connected to searches for BSM physics [14–16], future precision measurements from the EIC and Jefferson Lab sensitive to the transversity PDF are of utmost importance and necessary to see if a consistent picture emerges for the value of the tensor charge.

#### Acknowledgments

We would like to thank Haiyan Gao and Tianbo Liu for useful discussions about the SoLID pseudo-data. This work has been supported by the National Science Foundation under Grants No. PHY-1945471 (Z.K.), No. PHY-2011763 (D.P.), No. PHY-2012002 (A.P.), the U.S. Department of Energy, under contracts No. DE-FG02-07ER41460 (L.G.), No. DE-AC05-06OR23177 (A.P., N.S.) under which Jefferson Science Associates, LLC, manages and operates Jefferson Lab, and within the framework of the TMD Topical Collaboration. The work of N.S. was supported by the DOE, Office of Science, Office of Nuclear Physics in the Early Career Program.

#### References

- [1] J. P. Ralston and D. E. Soper, Nucl. Phys. **B152**, 109 (1979).
- [2] R. L. Jaffe and X.-D. Ji, Phys. Rev. Lett. **67**, 552 (1991).

- [3] R. L. Jaffe and X.-D. Ji, Nucl. Phys. **B375**, 527 (1992).
- [4] J. L. Cortes, B. Pire, and J. P. Ralston, Z. Phys. **C55**, 409 (1992).
- [5] L. P. Gamberg and G. R. Goldstein, Phys. Rev. Lett. **87**, 242001 (2001), hep-ph/0107176.
- [6] M. Anselmino *et al.*, Phys. Rev. **D87**, 094019 (2013), 1303.3822.
- [7] G. R. Goldstein, J. O. Gonzalez Hernandez, and S. Liuti, (2014), 1401.0438.
- [8] M. Radici, A. Courtoy, A. Bacchetta, and M. Guagnelli, JHEP **05**, 123 (2015), 1503.03495.
- [9] Z.-B. Kang, A. Prokudin, P. Sun, and F. Yuan, Phys. Rev. **D93**, 014009 (2016), 1505.05589.
- [10] M. Radici and A. Bacchetta, Phys. Rev. Lett. **120**, 192001 (2018), 1802.05212.
- [11] J. Benel, A. Courtoy, and R. Ferro-Hernandez, (2019), 1912.03289.
- [12] U. D'Alesio, C. Flore, and A. Prokudin, (2020), 2001.01573.
- [13] J. Cammarota *et al.*, Phys. Rev. D **102**, 054002 (2020), 2002.08384.
- [14] A. Courtoy, S. Baeßler, M. González-Alonso, and S. Liuti, Phys. Rev. Lett. **115**, 162001 (2015), 1503.06814.
- [15] T. Liu, Z. Zhao, and H. Gao, Phys. Rev. D **97**, 074018 (2018), 1704.00113.
- [16] M. González-Alonso, O. Naviliat-Cuncic, and N. Severijns, Prog. Part. Nucl. Phys. **104**, 165 (2019), 1803.08732.
- [17] N. Hasan *et al.*, Phys. Rev. **D99**, 114505 (2019), 1903.06487.
- [18] C. Alexandrou *et al.*, (2019), 1909.00485.
- [19] M. Pitschmann, C.-Y. Seng, C. D. Roberts, and S. M. Schmidt, Phys. Rev. **D91**, 074004 (2015), 1411.2052.
- [20] R. Gupta *et al.*, Phys. Rev. **D98**, 034503 (2018), 1806.09006.
- [21] HERMES, A. Airapetian *et al.*, Phys. Rev. Lett. **94**, 012002 (2005), hep-ex/0408013.
- [22] COMPASS, M. Alekseev *et al.*, Phys.Lett. **B673**, 127 (2009), 0802.2160.
- [23] HERMES, A. Airapetian *et al.*, Phys.Lett. **B693**, 11 (2010), 1006.4221.
- [24] The Jefferson Lab Hall A, X. Qian *et al.*, Phys.Rev.Lett. **107**, 072003 (2011), 1106.0363.
- [25] COMPASS, C. Adolph *et al.*, Phys. Lett. **B744**, 250 (2015), 1408.4405.
- [26] Jefferson Lab Hall A, Y. X. Zhao *et al.*, Phys. Rev. **C90**, 055201 (2014), 1404.7204.
- [27] HERMES, A. Airapetian *et al.*, (2020), 2007.07755.
- [28] Belle, R. Seidl *et al.*, Phys. Rev. **D78**, 032011 (2008), 0805.2975.
- [29] BaBar, J. P. Lees *et al.*, Phys. Rev. **D90**, 052003 (2014), 1309.5278.
- [30] BaBar, J. P. Lees *et al.*, Phys. Rev. **D92**, 111101 (2015), 1506.05864.
- [31] BESIII, M. Ablikim *et al.*, Phys. Rev. Lett. **116**, 042001 (2016), 1507.06824.
- [32] Belle, H. Li *et al.*, Phys. Rev. **D100**, 092008 (2019), 1909.01857.
- [33] STAR, L. Adamczyk *et al.*, Phys. Rev. **D97**, 032004 (2018), 1708.07080.
- [34] Z.-B. Kang, A. Prokudin, F. Ringer, and F. Yuan, Phys. Lett. **B774**, 635 (2017), 1707.00913.
- [35] U. D'Alesio, F. Murgia, and C. Pisano, Phys. Lett. **B773**, 300 (2017), 1707.00914.
- [36] Z.-B. Kang, K. Lee, and F. Zhao, Phys. Lett. B **809**, 135756 (2020), 2005.02398.
- [37] HERMES, A. Airapetian *et al.*, JHEP **06**, 017 (2008), 0803.2367.
- [38] COMPASS, C. Adolph *et al.*, Phys.Lett. **B713**, 10 (2012), 1202.6150.
- [39] COMPASS, C. Adolph *et al.*, Phys. Lett. **B736**, 124 (2014), 1401.7873.
- [40] COMPASS, C. Braun, EPJ Web Conf. **85**, 02018 (2015).
- [41] Belle, A. Vossen *et al.*, Phys. Rev. Lett. **107**, 072004 (2011), 1104.2425.
- [42] STAR, L. Adamczyk *et al.*, Phys. Rev. Lett. **115**, 242501 (2015), 1504.00415.
- [43] STAR, L. Adamczyk *et al.*, Phys. Lett. **B780**, 332 (2018), 1710.10215.
- [44] H.-W. Lin, W. Melnitchouk, A. Prokudin, N. Sato, and H. Shows, Phys. Rev. Lett. **120**, 152502 (2018), 1710.09858.
- [45] HERMES, A. Airapetian *et al.*, Phys. Rev. Lett. **103**, 152002 (2009), 0906.3918.
- [46] STAR, L. Adamczyk *et al.*, Phys. Rev. Lett. **116**, 132301 (2016), 1511.06003.
- [47] COMPASS, C. Adolph *et al.*, Phys. Lett. **B770**, 138 (2017), 1609.07374.
- [48] COMPASS, M. Aghasyan *et al.*, Phys. Rev. Lett. **119**, 112002 (2017), 1704.00488.
- [49] BRAHMS, J. H. Lee and F. Videbaek, AIP Conf. Proc. **915**, 533 (2007).
- [50] STAR, J. Adams *et al.*, Phys. Rev. Lett. **92**, 171801 (2004), hep-ex/0310058.
- [51] STAR, B. I. Abelev *et al.*, Phys. Rev. Lett. **101**, 222001 (2008), 0801.2990.
- [52] STAR, L. Adamczyk *et al.*, Phys. Rev. **D86**, 051101 (2012), 1205.6826.
- [53] J.-W. Qiu and G. Sterman, Phys. Rev. **D59**, 014004 (1998), hep-ph/9806356.
- [54] C. Kouvaris, J.-W. Qiu, W. Vogelsang, and F. Yuan, Phys. Rev. **D74**, 114013 (2006), hep-ph/0609238.
- [55] Y. Koike and T. Tomita, Phys. Lett. **B675**, 181 (2009), 0903.1923.
- [56] Z.-B. Kang, J.-W. Qiu, W. Vogelsang, and F. Yuan, Phys. Rev. **D83**, 094001 (2011), 1103.1591.
- [57] A. Metz and D. Pitonyak, Phys. Lett. **B723**, 365 (2013), 1212.5037.
- [58] H. Beppu, K. Kanazawa, Y. Koike, and S. Yoshida, Phys. Rev. **D89**, 034029 (2014), 1312.6862.
- [59] K. Kanazawa, Y. Koike, A. Metz, and D. Pitonyak, Phys. Rev. **D89**, 111501(R) (2014), 1404.1033.
- [60] L. Gamberg, Z.-B. Kang, D. Pitonyak, and A. Prokudin, Phys. Lett. **B770**, 242 (2017), 1701.09170.
- [61] A. Bacchetta *et al.*, JHEP **0702**, 093 (2007), hep-ph/0611265.
- [62] Y. V. Kovchegov and M. D. Sievert, Phys. Rev. **D99**, 054033 (2019), 1808.10354.
- [63] D. Boer *et al.*, (2011), 1108.1713.
- [64] A. Accardi *et al.*, Eur. Phys. J. **A52**, 268 (2016), 1212.1701.
- [65] J. Dudek *et al.*, Eur. Phys. J. **A48**, 187 (2012), 1208.1244.
- [66] SoLID, J. Chen, H. Gao, T. Hemmick, Z. E. Meziani, and P. Souder, (2014), 1409.7741.
- [67] Private communication with Haiyan Gao and Tianbo Liu.

- [68] E. Aschenauer *et al.*, pythiaerhic, 2020.
- [69] T. Sjostrand, S. Mrenna, and P. Z. Skands, *JHEP* **05**, 026 (2006), hep-ph/0603175.
- [70] T. Burton, A. Kisselev, K. Kauder, and M. Savastio, Eic-smear, 2020.
- [71] E. Aschenauer *et al.*, Electron-ion collider detector requirements and r&d handbook, v1.2, 2020.
- [72] M. Anselmino *et al.*, *Eur. Phys. J.* **A39**, 89 (2009), 0805.2677.
- [73] Belle-II, W. Altmannshofer *et al.*, *PTEP* **2019**, 123C01 (2019), 1808.10567.
- [74] A. Metz, *Phys. Lett.* **B549**, 139 (2002).
- [75] J. C. Collins and A. Metz, *Phys. Rev. Lett.* **93**, 252001 (2004), hep-ph/0408249.
- [76] L. P. Gamberg, A. Mukherjee, and P. J. Mulders, *Phys. Rev.* **D77**, 114026 (2008), 0803.2632.
- [77] F. Yuan, *Phys.Rev.Lett.* **100**, 032003 (2008), 0709.3272.
- [78] S. Meissner and A. Metz, *Phys. Rev. Lett.* **102**, 172003 (2009), 0812.3783.
- [79] L. P. Gamberg, A. Mukherjee, and P. J. Mulders, *Phys. Rev. D* **83**, 071503 (2011), 1010.4556.
- [80] D. Boer, Z.-B. Kang, W. Vogelsang, and F. Yuan, *Phys. Rev. Lett.* **105**, 202001 (2010), 1008.3543.
- [81] B.-T. Wang *et al.*, *Phys. Rev. D* **98**, 094030 (2018), 1803.02777.
- [82] I. Borsa, G. Lucero, R. Sassot, E. C. Aschenauer, and A. S. Nunes, *Phys. Rev. D* **102**, 094018 (2020), 2007.08300.